Dynamics of Sulfonated Polystyrene Ionomers Using Broadband Dielectric Spectroscopy

Pornpen Atorngitjawat and James Runt*

Department of Materials Science and Engineering and Materials Research Institute, The Pennsylvania State University, University Park, Pennsylvania 16802

Received July 6, 2006; Revised Manuscript Received December 13, 2006

ABSTRACT: The dynamics of sulfonated polystyrene ionomers were investigated by using broadband dielectric relaxation spectroscopy. Dynamic mechanical analysis, Fourier transform infrared spectroscopy, differential scanning calorimetry, and small-angle X-ray scattering were employed in a complementary role. Sulfonated polystyrene ionomers were prepared from the precursor sulfonic acid polystyrene, having 1 and 7 mol % sulfonic acid, by exchanging the protons of the acid functionality with Na, Cs, and Zn cations. Three dielectric relaxations were observed above the glass transition temperature: the segmental α process and relaxations associated with Maxwell−Wagner−Sillars interfacial polarization and electrode polarization. The low-frequency broadening of the α transition is related to constraints imposed by the ionic aggregates. A relaxation in the glassy state was observed for the precursor sulfonic acid polystyrene and ionomers and attributed to the local motion of sulfonated phenyl groups. The relaxation strengths of the β processes of the ionomers were suppressed by interaction with the cations that create physical cross-links, and the relaxation times decreased with increasing strength of the electrostatic interaction of the ion pairs.

1. Introduction

Ionomers are nominally random copolymers that consist of a hydrocarbon backbone and a relatively small fraction (ca. $<\sim$10%) of pendent groups with acid functionality, neutralized partially or completely with cations.[1,2] They are high-performance materials that display marked improvement over the acid form of the parent copolymers in electrolytic transport and physical properties, such as conductivity, modulus, adhesive strength, and impact strength. Enhancements in mechanical properties result primarily from the aggregation of ionic species into clusters, which serve as physical cross-links.[3]

During the past 30 years there have been a number of studies of ionomer morphology by techniques such as small-angle X-ray scattering (SAXS),[4−14] transmission electron microscopy (TEM),[14−18] and dynamic mechanical analysis (DMA).[6,19−22] However, there have been few systematic investigations of the dynamic relaxation behavior of amorphous ionomers using dielectric relaxation spectroscopy (DRS) and none on sulfonated polystyrene (SPS) ionomers that we are aware of. DRS is powerful tool for understanding the influence of ions on segmental and local motions as well as aggregate dynamics. We have chosen SPS ionomers as a model system since there is no crystallinity, and neat polystyrene (PS) provides a relatively dielectrically inactive background signal for more ready identification of the dynamics of the sulfonated groups. In a recent paper, we reported an analysis of the dielectric relaxation behavior of the precursor SPS copolymers in acid form. Particularly noteworthy was the observation of an α* relaxation, arising from the association and dissociation of hydrogen bonds.[3] In the current paper, we investigate the dynamics of SPS ionomers, neutralized with Na^+, Cs^+, and Zn^{2+} using broadband DRS. The findings are interpreted with the assistance of complementary Fourier transform infrared (FTIR) spectroscopy, differential scanning calorimetry (DSC), SAXS, and DMA experiments.

* Corresponding author. E-mail: runt@matse.psu.edu.

2. Experimental Section

2.1. Materials and Sample Preparation. Neutralization of Sulfonated Polystyrene. The precursor sulfonic acid polystyrenes (SPS-H), having 1 and 7 mol % sulfonic acid functionality, were prepared as described in a previous paper.[3] Neutralization was accomplished as described in the literature.[23] The acid form of the appropriate SPS copolymer was dissolved in chloroform. A measured amount of sodium hydroxide, zinc acetate, or cesium hydroxide was dissolved in methanol/water (2:1) and added to the SPS-H solution with stirring for 5 h at 60 °C under flowing N_2 gas. The neutralized sulfonated polystyrenes (SPS-M) were precipitated with ethanol, followed by washing with hot water and methanol, filtered, and dried under vacuum at 100 °C for 48 h before sample preparation.

Degree of Neutralization. Degrees of neutralization were estimated by measuring the remaining acid content of the materials via a titration method, as described in our previous paper.[3] The percent neutralization is presented in Table 1. The degrees of neutralization of all ionomers are ca. ∼90%. Sulfonation levels of the two SPS-H studied were 1.1 and 6.8 mol %.[3] The unneutralized SPS are referred to as SPS1H and SPS7H, respectively, and the neutralized versions of these polymers are referred to as SPS1Na, SPS7Na, SPS7Cs, and SPS7Zn.

Water Content. The water content of the SPS ionomers was measured using a coulometric Karl Fischer titration method (KF titration). Hydranal CG and Hydranal A were used as catholyte and anolyte reagents.[3] The water content of all SPS ionomers, before and after DRS experiments, was found to be less than 0.3 wt %.

2.2. Experimental Methods. Sample films of 0.1−0.3 mm thickness were prepared by solution casting from dimethylformamide (DMF), for DSC, DMA, and DRS characterization. To facilitate solvent and water removal, films were heated to 120 °C under vacuum for at least 24 h.

Differential Scanning Calorimetry. Glass transition temperatures (T_g) were determined using a TA Q-100 DSC. Temperature and transition enthalpy were calibrated using an indium standard. The samples were in film form and weighed from 8 to 10 mg. Samples were first heated from 20 to 140 °C at a heating rate of 10 °C/min, held for 5 min, and then cooled at 40 °C/min to 20 °C. After holding for 3 min, samples were reheated to 250 °C at a

10.1021/ma061516r CCC: $37.00
Published on Web 01/23/2007

Table 1. Sulfonation Levels, Degree of Neutralization, and T_gs of SPS-H and SPS-M

sample	sulfonation level (mol %)	degree of neutralization (%)	T_g (°C)
SPS7H	6.8	0	110
SPS1H	1.1	0	106
SPS1Na	1.1	90	106
SPS7Na	6.8	86	116
SPS7Cs	6.8	86	117
SPS7Zn	6.8	89	115

heating rate of 10 °C/min. Results shown in this paper are taken from the last step.

Fourier Transform Infrared Spectroscopy. Infrared spectra were acquired using a Bio-Rad FTS-6 spectrometer, signal averaging 128 scans at a resolution of 2 cm^{-1}. Sample solutions were deposited to KBr windows, and the solvent evaporated at room temperature, followed by gradually heating to 120 °C and then maintaining at 120 °C under vacuum for 24 h.

Dynamic Mechanical Analysis. Dynamic mechanical properties in tensile mode were performed using a TA Q-800 DMA, at frequency of 1 Hz and a heating rate of 5 °C/min. The storage (E') and loss moduli (E'') were determined as a function of temperature (from 50 up to 300 °C) for rectangular films (18 mm by 5 mm by 0.1−0.3 mm).

Small-Angle X-ray Scattering. SAXS profiles were collected using a two-dimensional detector, and the scattering vector was calibrated with silver behenate. A parallel ionization detector was placed in front of the samples to record the incident and transmitted intensities. The sample-to-detector distance was 1.5 m. Data were acquired for 2 h and azimuthally averaged to yield a one-dimensional profile of intensity $I(q)$ vs scattering vector q ($q = (4\pi/\lambda)\sin\theta$, where λ is the X-ray wavelength and 2θ is the scattering angle).

Broadband Dielectric Relaxation Spectroscopy. Dielectric relaxation spectra were collected isothermally using a Novocontrol GmbH Concept 40 broadband dielectric spectrometer in the frequency domain from 0.01 Hz to 1 MHz in the range 30−220 °C. Temperature stability was controlled within ±0.2 °C. Sample films were sputtered with gold, covered by silver sheets, and tightly sandwiched between electrodes of 2 cm diameter.

3. Results and Discussion

3.1. DSC. A single glass transition (T_g) was observed for all SPS ionomers. A second higher temperature transition is not detected (however, see discussion of DMA results to follow). This is not surprising since similar behavior has been reported by many other groups.[12,19,22,24,25] The T_g of SPS7Na is higher than SPS1Na due to the higher degree of sulfonation (Table 1). T_gs of the SPS7-M ionomers are slightly higher than SPS7H resulting from physical cross-linking, and no effect of counterion type on T_g was observed at the same sulfonation level.[19,22,24,25]

3.2. FTIR. Figure 1 displays FTIR spectra of SPS7H and the corresponding ionomers between 950 and 1300 cm^{-1}. The arrows denote the positions of the bands associated with sulfonated species in proximity to the cations. The band assignments are provided in Table 2.[26,27] As seen in Figure 1, the doublet at ~1200 cm^{-1} and the absorption at 1042 cm^{-1} are attributed to the antisymmetric and symmetric stretching vibration of the S−O bond of the $-SO_3^-M^+$, respectively. The bands at 1128 and 1011 cm^{-1} result from the in-plane skeletal vibration of benzene rings substituted by SO_3^- and SO_3M, respectively.[26,27] The splitting of the antisymmetric stretching vibration is due to either cations polarizing the anion asymmetrically or cations located on a single oxygen atom (see Table 2).[26,27] Furthermore, the FTIR spectra permit an estimate of the energy of ion pairs; the greater the strength of the electrostatic interaction of a given ion pair, the larger the splitting of

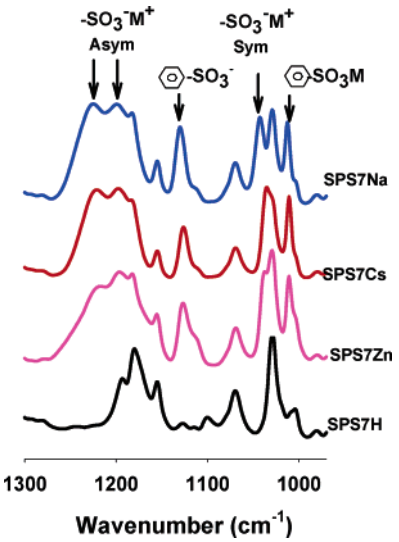

Figure 1. FTIR spectra of SPS7H, SPS7Na, SPS7Cs, and SPS7Zn.

Table 2. FTIR Absorption Peaks and Assignments of SPS-M[26,27]

Absorbance band	SPS1Na	SPS7Na	SPS7Cs	SPS7Zn
$SO_3^-M^+$, sym	1040	1042	1033	1039
$SO_3^-M^+$, asym	1226	1225	1220	1221
	1199	1199	1199	1193
SO_3^-	1128	1128	1127	1128
SO_3M	1012	1011	1011	1011

antisymmetric stretching vibration.[26,28] Our results show a small difference in splitting, which leads to estimates of the electrostatic interaction strength of the ion pairs in the series $Zn^{2+} > Na^+ > Cs^+$.[26]

3.3. DMA. Figure 2 displays storage and loss moduli as a function of temperature for the SPS ionomers, compared with to the behavior of SPS7H. Results from DMA are not compared directly to those from dielectric measurements since the DMA frequency window is relatively small (0.01−100 Hz), and temperature scans are typical and were employed here. DMA is used in the current work to assist in assigning DRS relaxation processes (see section 3.5).

All ionomers exhibit a rubbery plateau (Figure 2a) above the temperature of the α process, as expected for systems in which ionic clusters provide physical cross-links. The plateau moduli of SPS7Na and SPS7Cs are higher than SPS7Zn, indicating that the distance between physical cross-links increases for divalent cations[29] and the lower ionic strength of Na^+ and Cs^+.[22] The rubbery plateau of SPS7Zn is slightly longer than SPS7Na and considerably longer than SPS7Cs.[21] This is consistent with the relative strengths of ion pairs in the ionic aggregates of $Zn^{2+} > Na^+ > Cs^+$ [21,22] and in keeping with the FTIR results discussed above. Loss modulus spectra (Figure 2b) clearly show two transitions for all SPS ionomers. In contrast, no transition at temperatures above the mechanical α relaxation, associated with segmental motion, was observed for SPS7H.[3] The high-temperature transitions have been proposed to arise from segmental motions under constraint from ionic aggregates and have been referred to as α_2 relaxations.[6,19−22] The approximate magnitudes of the α_2 relaxations of SPS7Na and SPS7Cs are higher than that of SPS7Zn, and it has been proposed that chain segments attached to ionic clusters in SPS7Na and SPS7Cs are less restricted than those in SPS7Zn.[29]

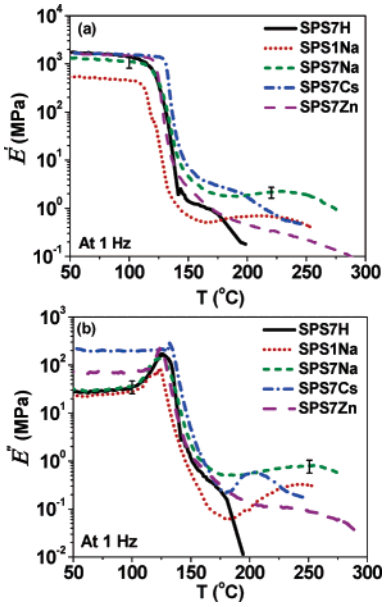

Figure 2. (a) Storage and (b) loss moduli vs temperature for SPS7H, SPS1Na, SPS7Na, SPS7Cs, and SPS7Zn at 1 Hz. The error bars represent the 95% confidence interval for the data of all samples.

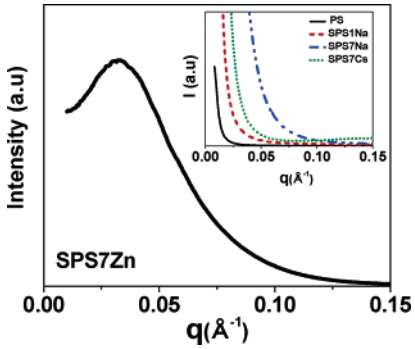

Figure 3. SAXS profile of SPS7Zn measured at room temperature. Inset: SAXS profile for PS, SPS1Na, SPS7Na, and SPS7Cs at room temperature.

3.4. SAXS. It has been demonstrated in previous SAXS studies of ionomers that the resulting scattering (phase-separated morphology) depends strongly on the method of sample preparation and thermal history.[6,11,12,14] We observe an "ionomer scattering peak" for SPS7Zn at $q = 0.04$ Å^{-1} (Figure 3), which is attributed to the presence of ionic aggregates in the PS matrix.[5,6] The mean interdomain spacing for SPS7Zn prepared in this way is ~15 nm.[14] However, no such scattering peak was observed for SPS7Cs, SPS7Na, or SPS1Na, although the scattering at very small angles is much greater than that of neat PS (see the inset in Figure 3).[11−13] [The upturn in the scattering of PS below $q \sim 0.02$ is due to spillover from the beamstop, which also seen with no sample in the holder.] Similar results have been reported previously, and it has been proposed that the small-angle upturn is associated with long-range inhomogeneity of the metal ions.[11−13] Some earlier investigations of Cs and Na forms of SPS ionomers[2,6] reported SAXS "ionomer peaks" at $q \sim 0.17-0.18$ Å^{-1}, but due to the higher angular detector limit of our SAXS experiments, we were unable to interrogate the scattering above 0.15 Å^{-1}. In addition, only amorphous halos were observed for all samples by wide-angle X-ray diffraction (WAXD) although the angular range of the WAXD experiments did not overlap with that of SAXS.

3.5. DRS. Segmental α Process. The segmental relaxation times and dielectric relaxation strengths of PS, unneutralized SPS, and the SPS ionomers were obtained by fitting the isothermal dielectric loss $\epsilon''(f)$ curves with the Havriliak−Negami (HN) function,[30] together with a contribution to the loss from dc conductivity when appropriate:

$$\epsilon^*(\omega) = \epsilon'(\omega) - i\epsilon''(\omega) = \epsilon_\infty - i\frac{\sigma_0}{(\epsilon_0\omega)^s} + \sum \frac{\Delta\epsilon}{[1 + (i\tau_{HN}\omega)^m]^n} \quad (1)$$

where ϵ^*, ϵ', and ϵ'' are the complex, real, and imaginary components of the dielectric permittivity, respectively; the relaxation strength, $\Delta\epsilon$, $= \epsilon_\infty - \epsilon_s$, where ϵ_∞ and ϵ_s are the dielectric constants at limiting high and low frequencies, respectively; σ_0 is the dc conductivity (S/cm); ω is the angular frequency; τ_{HN} is the characteristic relaxation time; and m and n are relaxation shape parameters, indicative of the breadth of the relaxation and peak asymmetry, respectively. The exponent s in the dc conduction contribution (i.e., the second term on the right-hand side of eq 1) characterizes the nature of the conduction process. See for example Figure 4, which shows dielectric loss spectra of SPS7Zn, after subtraction of conduction losses, at several temperatures. The segmental relaxation times (τ_{max}) of all samples follow a Vogel−Fulcher−Tammann (VFT) form,[31] as expected (see Figure 5). The VFT expression is

$$\tau_{max} = \tau_0 \exp\left(\frac{B}{T - T_0}\right) \quad (2)$$

where τ_0 and B are constants. τ_0 is sometimes associated with vibration lifetimes, B is related to the apparent activation energy,[32] and T_0 is the Vogel temperature, below which segments become immobile. Fitting the VFT expression to the

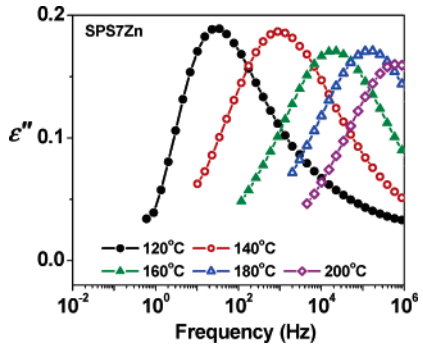

Figure 4. Dielectric loss spectra of SPS7Zn, after subtraction of conduction losses, at selected temperatures.

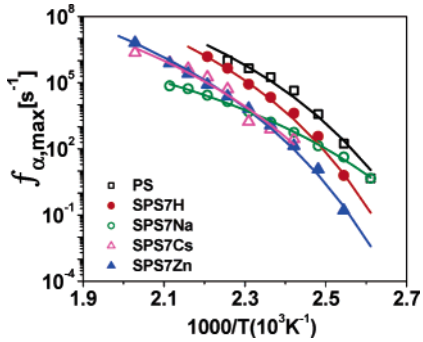

Figure 5. Relaxation times of the α process as a function of temperature for PS, SPS7H, SPS7Na, SPS7Cs, and SPS7Zn. Solid lines indicate VFT fits to the data.

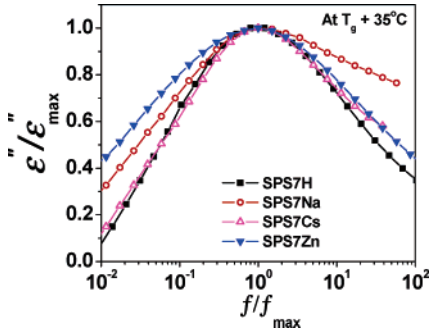

Figure 6. Normalized (by ϵ''_{max} and f_{max}) dielectric α processes of SPS7H, SPS7Na, SPS7Cs, and SPS7Zn at T_g + 35 °C.

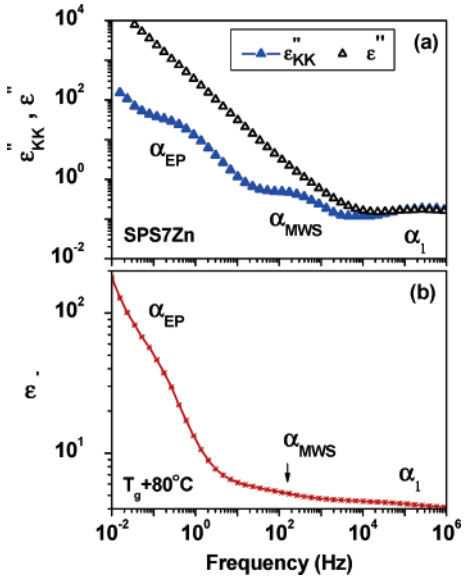

Figure 7. Dielectric spectrum of SPS7Zn at T_g + 80 °C: (a) the dielectric loss ϵ'' (open symbols) compared with the calculated ϵ''_{KK} (filled symbols) spectrum and (b) the dielectric constant ϵ' spectrum.

data for the SPS ionomers (using a constant $\tau_0 = 10^{-14}$ s) yields values of B between 0.19 and 0.29 eV and T_0 between 12 and 35 °C. Similar to our earlier results on the influence of hydrogen bonding on the segmental dynamics of SPS7H, the intermolecular cooperativity of SPS ionomers is not significantly affected by the physical cross-linking imparted by the ion clusters.[3]

A comparison of the dielectric α (α_1) processes of the ionomers and unneutralized SPS at T_g + 35 °C is displayed in Figure 6. The slight broadening at low frequencies for SPS7Zn and SPS7Na is likely due to constraints associated with the ionic aggregates. The high-frequency broadening of SPS7Cs, and particularly SPS7Na, arises from overlap with local processes. While the dielectric α relaxation strengths, $\Delta\epsilon(\alpha)$, of SPS7H and the ionomers change insignificantly over the temperature range investigated, $\Delta\epsilon(\alpha)$ at T_g + 80 °C varies significantly between materials: the strength of the α process for SPS7H (0.71) is significantly higher than that of SPS7Zn (0.49), SPS7Na (0.44), and SPS7Cs (0.33). $\Delta\epsilon(\alpha)$[SPS7H] contains a contribution from the polar acid groups, and although there is a small quantity of unneutralized acid remaining in the ionomers and likely some neutralized species remaining in the matrix phase, clustering occurs and inhibits movement of some segments in or near clusters. Such segments presumably relax at much higher temperatures, i.e., are associated with the mechanical α_2 process. As noted below, α_2 processes were only observed in DMA experiments, not dielectric. The α_2 processes

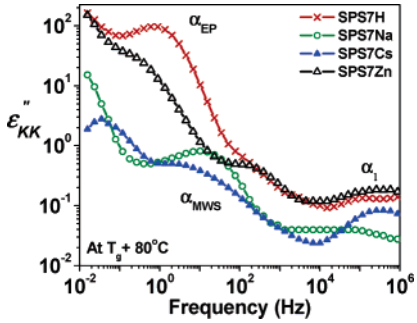

Figure 8. ϵ''_{KK} spectra vs frequency at T_g + 80 °C of SPS7H, SPS7Na, SPS7Cs, and SPS7Zn, indicating the segmental (α), Maxwell−Wagner-Sillars (α_{MWS}), and electrode polarization (α_{EP}) processes.

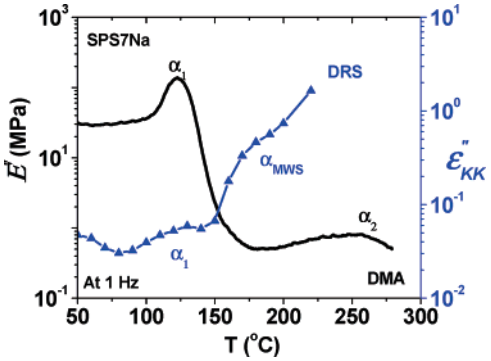

Figure 9. Cross plot of dynamic mechanical and dielectric loss ϵ''_{KK} as a function of temperature for SPS7Na at 1 Hz.

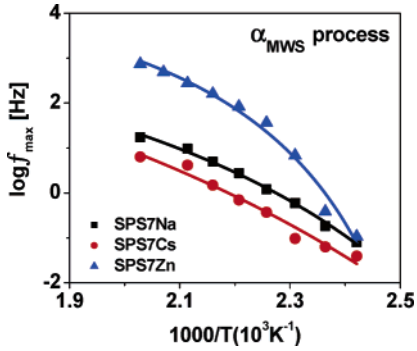

Figure 10. Relaxation times of the α_{MWS} process as a function of temperature for SPS7Na, SPS7Cs, and SPS7Zn.

cannot be observed in dielectric spectra, even in the Kramers−Kronig transformed spectra discussed below, since they are overwhelmed by the contribution of electrode polarization to ϵ'' and ϵ' at temperatures of 200 °C and above.

The dielectric loss ϵ'' was also obtained by transforming the dielectric constant ϵ' via a numerical version of the Kramers−Kronig (KK) transform (eq 3) and is symbolized as ϵ''_{KK}:[33]

$$\epsilon''_{KK}(\omega_0) = \frac{\sigma_0}{\epsilon_v \omega_0} + \frac{2}{\pi}\int_0^\infty \epsilon'(\omega)\frac{\omega}{\omega^2 - \omega_0^2}\,d\omega \qquad (3)$$

where ϵ_v refers to the vacuum permittivity and ω_0 is the angular frequency of the electric field. This numerical technique provides the advantage of suppressing ohmic conduction since it is removed by the KK transform.[33] The KK transform used here utilizes an eight-point numerical method and the coefficients developed by Steeman and van Turnhout.[34] This is particularly helpful for identifying dipole relaxations in regions of dielectric loss spectra having high conduction losses. For example, ϵ'', ϵ''_{KK}, and ϵ' spectra of SPS7Zn at T_g + 80 °C are compared in

Table 3. Dielectric Relaxation Strength of the α, α_{MWS}, and α_{EP} Processes and the Activation Energy of the α Process at T_g + 80 °C for SPS7M

sample	$\Delta\epsilon(\alpha)$	$\Delta\epsilon(\alpha_{MWS})$	$\Delta\epsilon(\alpha_{EP})$	$E_a(\alpha)$ [kJ/mol]
SPS7Na	0.44	1.85	10.5	184
SPS7Cs	0.33	1.32	5.3	189
SPS7Zn	0.49	0.95	67	191

Table 4. Dielectric Relaxation Strength, Relaxation Shape Parameters, and Activation Energy of the β Relaxations at 60 °C of SPS-H and SPS-M

sample	$\Delta\epsilon(\beta)$	*mn*	$E_a(\beta)$ [kJ/mol]
SPS7H	0.55	0.18	69
SPS7Na	0.34	0.55	76
SPS7Cs	0.41	0.23	35
SPS7Zn	0.26	0.82	34

Figure 7 (SPS7Cs, SPS7Na, and SPS1Na are similar and not shown). We clearly observe two additional relaxation processes at temperatures above the dielectric α relaxation for all ionomers, as demonstrated in Figure 8. Their proposed origin is described below.

α_{EP} Process. The high loss and dielectric constant associated with the highest temperature−low frequency process clearly identifies it as originating from electrode polarization (EP), which arises from the accumulation of mobile ions at electrode interfaces (see Figure 7, for SPS7Zn).[3,35] Because of the relatively high T_gs of the SPS ionomers, α_{EP} was only observed in a temperature range from 190 to 220 °C.

α_{MWS} Process. This process is located between the dielectric α and α_{EP} processes, and it might at first seem reasonable to assign it to motions analogous to the DMA α_2 relaxation. However the DMA α_2 process is observed at a much higher temperature (50−70 °C higher) at the same frequency (see the isochronal plot in Figure 9, for example). As noted earlier, there is a very small amount (<0.3 wt %) of residual water in the samples, presumably in "bound" form, but there is no evidence in the literature for a relaxation for bound water in the frequency range of our measurements. Therefore, since many previous findings as well as those in the present paper support the two-phase nature of SPS ionomers, we propose that this process is a manifestation of Maxwell−Wagner−Sillars (MWS) interfacial polarization, which arises in multiphase systems in which the phases have different dielectric constants and conductivities.[23]

The dielectric relaxation strengths of the α, α_{MWS}, and α_{EP} processes and the activation energy of the segmental process at T_g + 80 °C are provided in Table 3. From eq 2, the apparent α activation energy is obtained as $E_{app}(T) = B/(1 - T_0/T)^2$.[32] E_a for α_{MWS} (~100 kJ/mol) and α_{EP} are not included in Table 3 because they are not physically meaningful. The MWS relaxation times for SPS7Zn exhibit a non-Arrhenius temperature dependence, as shown in Figure 10, but the form of the temperature dependence for SPS7Na and SPS7Cs is uncertain due to the relative lack of data points. The α_{MWS} relaxation times for SPS1Na are not shown since the strength of the α_{MWS} process is quite small for this material (consistent with its assignment as an MWS process), and at some temperatures it overlaps with the segmental process. Finally, although in principle one can use the characteristics of the observed MWS processes to extract information about the nature of the phase-separated clusters, the MWS models needed to do so have too many unknown parameters to make this a worthwhile exercise.

Local β Relaxations. Unlike neat PS, SPS7H and its Na, Cs, and Zn ionomers exhibit relatively weak β relaxations (Figure 11). This process is not associated with residual water as we pointed out in ref 3. Even when samples were soaked in water (reaching ~2% water content), the relaxation time and strength of the β process remained unchanged. A new relaxation did appear at lower frequencies in this temperature range but disappeared upon heating above 120 °C.

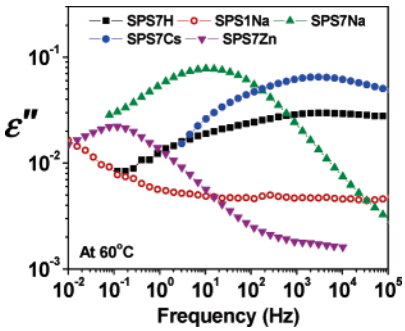

Figure 11. Dielectric loss spectra for SPS7H, SPS1Na, SPS7Na, SPS7Cs, and SPS7Zn at 60 °C.

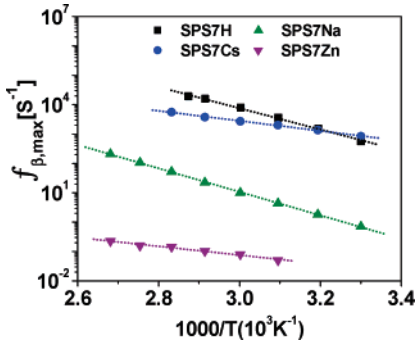

Figure 12. Temperature dependence of the relaxation times for the β processes of SPS7H, SPS7Na, SPS7Cs, and SPS7Zn. The dotted line represents an Arrhenius fit.

Therefore, we assigned the β process to the motion of the sulfonated phenyl groups in the glassy state.[3] SPS1Na exhibits a very weak β relaxation due to the small amount of sulfonation (1 mol %). The β relaxation strengths $\Delta\epsilon(\beta)$, the shape parameters, and the activation energies of SPS7Na, SPS7Cs, SPS7Zn, and SPS7H, are displayed in Table 4. $\Delta\epsilon(\beta)$ decreases in the order SPS7H > SPS7Cs > SPS7Na > SPS7Zn, suggesting that this local motion is suppressed in the ionomers by interaction with the cations that create the physical cross-links. Furthermore, the relaxation times of the β process decrease as SPS7H > SPS7Cs > SPS7Na > SPS7Zn, as seen in Figure 12. The sequence of decreasing relaxation strengths and times follows the increased electrostatic interaction energy of the ion pairs. The activation energies shown in Table 4 do not follow a trend based on ionic strengths.

4. Summary

The single glass transitions of SPS ionomers were observed to increase slightly from that of unneutralized SPS due to physical cross-links created by ionic aggregates. FTIR and DMA results demonstrated qualitatively similar trends with the strength of the electrostatic interaction of the ion pairs in ionomers. The ionomers also exhibited a rubbery plateau in DMA experiments and a second transition above the mechanical α relaxation for all SPS ionomers, attributed to segmental motion under relatively severe constraint from the physical cross-links. The mean interdomain spacing for SPS7Zn observed from SAXS was ~15 nm. The large upturn in scattering intensity at small angles for the ionomers has been proposed previously to be associated with the long-range inhomogeneity of the metal ions.

The dielectric spectra of the SPS ionomers revealed four relaxation processes. Three of these are observed above the glass

transition temperature and attributed to the segmental relaxation (α) and processes arising from Maxwell−Wagner−Sillars interfacial polarization and electrode polarization. The relaxation strength of the segmental α process of the SPS ionomers was found to be significantly lower than SPS7H due to the reduction in polar acid species and constraints imparted by physical cross-links.

A local dielectric β process was observed for SPS and the ionomers and assigned to the motion of sulfonated phenyl groups. The reduction in relaxation strength and slowing down of the β process demonstrated the effect of physical cross-links on decreasing the mobility of the sulfonated phenyl groups.

Acknowledgment. The authors thank the National Science Foundation, Polymers Program (DMR-0605627), for partial support of this research. P.A. expresses her appreciation to the Royal Thai Government for financial support. We also thank Robert Klein for providing the KK transform program and his helpful discussions. Finally, we also thank Prof. Paul Painter for very helpful discussions.

References and Notes

(1) Schlick, S., Ed. *Ionomers: Characterization, Theory, and Applications*; CRC Press: New York, 1996.
(2) Utracki, L. A.; Weiss, R. A. *Multiphase Polymers: Blends and Ionomers*; American Chemical Society: Washington, DC, 1989.
(3) Atorngitjawat, P.; Klein, J. R.; Runt, J. *Macromolecules* **2006**, *39*, 1815.
(4) Eisenberg, A.; Hird, B.; Moore, R. B. *Macromolecules* **1990**, *23*, 4098.
(5) Yarusso, D. J.; Cooper, S. L. *Macromolecules* **1983**, *16*, 1871.
(6) Weiss, R. A.; Lefelar, J. A. *Polymer* **1986**, *27*, 3.
(7) Fujimura, M.; Hashimoto, T.; Kawai, H. *Macromolecules* **1981**, *14*, 1309.
(8) Sauer, B. B.; Mclean, R. S. *Macromolecules* **2000**, *33*, 7939.
(9) Tsujita, Y.; Yasuda, M.; Kinoshita, T.; Takizawa, A.; Yoshimizu, H. *Macromolecules* **2001**, *34*, 2220.
(10) Tsujita, Y.; Yasuda, M.; Kinoshita, T.; Takizawa, A.; Yoshimizu, H.; Davies, G. R. *J. Polym. Sci., Polym. Phys.* **2002**, *40*, 831.
(11) Li, Y.; Peiffer, D. G.; Chu, B. *Macromolecules* **1993**, *26*, 4006.
(12) Galambos, A. F.; Stockton, W. B.; Koberstein, J. T.; Sen, A.; Weiss, R. A. *Macromolecules* **1987**, *20*, 3091.
(13) Wu, D. Q.; Phillips, J. C.; Lundberg, R. D.; Macknight, W. J.; Chu, B. *Macromolecules* **1989**, *22*, 992.
(14) Bata, A.; Cohen, C.; Kim, H.; Winey, K. I.; Ando, N.; Gruner, S. M. *Macromolecules* **2006**, *39*, 1630.
(15) Li, C.; Register, R. A.; Cooper, S. L. *Polymer* **1989**, *30*, 1227.
(16) Handlin, D. L.; MacKnight, W. J.; Thomas, E. L. *Macromolecules* **1981**, *14*, 795.
(17) Kirkmeyer, B. P.; Weiss, R. A.; Winey, K. I. *J. Polym. Sci., Polym. Phys.* **2001**, *39*, 477.
(18) Han, S. I.; Kang, S. W.; Kim, B. S.; Im, S. S. *Adv. Funct. Mater.* **2005**, *15*, 367.
(19) Weiss, R. A.; Fitzgerald, J. J.; Kim, D. *Macromolecules* **1991**, *24*, 1071.
(20) Eisenberg, A.; Navratil, M. *Macromolecules* **1973**, *6*, 604.
(21) Hara, M.; Jar, P.; Sauer, J. A. *Polymer* **1991**, *32*, 1622.
(22) Fan, X. D.; Bazuin, C. G. *Macromolecules* **1995**, *28*, 8216.
(23) Weiss, R. A.; Sen, A.; Willis, C. L.; Pottick, L. A. *Polymer* **1991**, *32*, 1867.
(24) Li, H.-M.; Liu, J.-C.; Zhu, F.-M.; Lin, S.-A. *Polym. Int.* **2001**, *50*, 421.
(25) Lu, X.; Weiss, R. A. *Macromolecules* **1992**, *25*, 6185.
(26) Zundel, G. *Hydration and Intermolecular Interaction: Infrared Investigations with Polyelectrolyte Membranes*; Academic Press: New York, 1969.
(27) Fitzgerald, J. J.; Weiss, R. A. *Coulombic Interactions in Macromolecular Systems*; American Chemical Society: Washington, DC, 1986; Chapter 3, p 35.
(28) Chen, W.; Sauer, J. A.; Hara, M. *Polymer* **2003**, *44*, 7729.
(29) Murayama, T. *Dynamic Mechanical Analysis of Polymeric Material*; Elsevier North-Holland: New York, 1978; Chapter 11, p 63.
(30) Havriliak, S.; Negami, S. *J. Polym. Sci., Polym. Symp.* **1966**, *14*, 99.
(31) Angell, C. A. *Polymer* **1997**, *38*, 6261.
(32) van Turnhout, J.; Wubbenhorst, M. *J. Non-Cryst. Solids* **2002**, *305*, 50.
(33) Wubbenhorst, M.; van Turnhout, J. *J. Non-Cryst. Solids* **2002**, *305*, 40.
(34) Steeman, P. A. M.; van Turnhout, J. *Colloid Polym. Sci.* **1997**, *275*, 106.
(35) Klein, R.; Zhang, S.; Dou, S.; Jones, B. H.; Colby, R. H.; Runt, J. *J. Chem. Phys.* **2006**, *124*, 144903.

MA061516R